Electroorganic Synthesis in Aqueous Solution via Generation of Strongly Oxidizing and Reducing Intermediates

Seyyedamirhossein Hosseini,[a] Joshua A. Beeler,[a] Melanie S. Sanford,[b*] Henry S. White[a*]

Affiliation:

[*] Corresponding author: white@chemistry.utah.edu; mssanfor@umich.edu

[a] Department of Chemistry, University of Utah, 315 S 1400 E Salt Lake City, Utah 84112, United States

[b] Department of Chemistry, University of Michigan, 930 North University Avenue, Ann Arbor, Michigan 48109, United States

Water is the ideal green solvent for organic electrosynthesis. However, a majority of electroorganic processes require potentials that lie beyond the electrochemical window for water. In general, water oxidation and reduction lead to poor synthetic yields and selectivity or altogether prohibit carrying out a desired reaction. Herein, we report several electroorganic reactions in water using synthetic strategies referred to as *reductive oxidation* and *oxidative reduction*. Reductive oxidation involves the homogeneous reduction of peroxydisulfate ($S_2O_8^{2-}$) via electrogenerated $Ru(NH_3)_6^{2+}$ at potential of –0.2 V vs. Ag/AgCl (3.5 M KCl) to form the highly oxidizing sulfate radical anion ($E^{0'}$ ($SO_4^{\bullet-}/SO_4^{2-}$) = 2.21 V vs. Ag/AgCl), which is capable of oxidizing species beyond the water oxidation potential. Electrochemically generated $SO_4^{\bullet-}$ then efficiently abstracts a hydrogen atom from a variety of organic compounds such as benzyl alcohol and toluene to yield product in water. The reverse analogue of reductive oxidation is oxidative reduction. In this case, the homogeneous oxidation of oxalate ($C_2O_4^{2-}$) by electrochemically generated $Ru(bpy)_3^{3+}$ produces the strongly reducing carbon dioxide radical anion ($E^{0'}$ ($CO_2^{\bullet-}/CO_2$) = –2.1 V vs. Ag/AgCl), which can reduce species at potential beyond the water or proton reduction potential. In preliminary studies, the

$CO_2^{\bullet-}$ has used to homogenously reduce the C–Br moiety belonging to benzyl bromide at an oxidizing potential in aqueous solution.

Introduction

A goal of chemical industries is to develop processes that can be performed in aqueous solution. Besides intrinsic greenness, several features such as abundance and minimal solvent handling makes water a very appealing solvent. In this context, developing electroorganic reactions that can be carried out in an aqueous solution is a very attractive idea. In comparison to popular organic solvents such as dimethyl formamide (DMF) and acetonitrile (MeCN), water has a large dielectric constant allowing for the use of common inorganic supporting electrolytes and reagents at high concentrations. However, in general, electroorganic reactions in an aqueous solution are limited by the small potential window of water, which is defined as the potentials beyond which water undergoes direct reduction and oxidation (i.e., eqs. 1 and 2).[1, 2]

$2H_2O + 2e^- \rightleftharpoons H_2 + 2OH^-$ $E^0 = -1.1$ V vs. Ag/AgCl (3.5 M KCl) (alkaline solution) (1)

$2H_2O \rightleftharpoons 4H^+ + O_2 + 4e^-$ $E^0 = 1.03$ V vs. Ag/AgCl (3.5 M KCl) (acidic solution) (2)

The majority of the electroorganic reactions, such as the electrochemical reduction of C–X (X = Cl, Br, I) or electrochemical C–H oxidation, require the application of potentials beyond the water potential window.[3] Therefore, water reduction/oxidation interferes with electroorganic reactions, yielding undesirable side products and low reaction yields.

In a recent report, we have proposed that the electrogeneration of highly oxidizing/reducing intermediates from water soluble reagents, and interception of these transient species by organic compounds, provides a promising approach to perform electroorganic reactions that would

normally be prohibited by the oxidation or reduction of water.[12] Electrogeneration of highly oxidizing and reducing intermediates was developed by Bard and coworkers to create excited state species in aqueous solutions that emitted light, a process referred to as electrogenerated chemiluminescence or ECL.[4] In particular, two approaches for generating ECL are based on: (1) $S_2O_8^{2-}$ reduction to generate the strong oxidant, $SO_4^{\bullet-}$ and (2) $C_2O_4^{2-}$ oxidation to generate the strong reductant, $CO_2^{\bullet-}$.[4–6] In the present work, we employed $S_2O_8^{2-}$ reduction and $C_2O_4^{2-}$ oxidation as the initial steps in performing synthetic organic reactions in aqueous solutions.

Figure 1 shows the cyclic voltammogram for the direct reduction of $S_2O_8^{2-}$ (red trace) and oxidation of $C_2O_4^{2-}$ (blue trace) at a glassy carbon (GC) electrode. Briefly, the one-electron reduction of $S_2O_8^{2-}$ generates $S_2O_8^{3\bullet-}$, which rapidly dissociates to form SO_4^{2-} and the highly oxidizing sulfate radical anion ($E^{0\prime}$ ($SO_4^{\bullet-}/SO_4^{2-}$) = 2.21 V vs. Ag/AgCl (3.5 M KCl).[5-7] Electrogenerated $SO_4^{\bullet-}$ can be further reduced at the working electrode. Alternatively, $SO_4^{\bullet-}$ can accept an electron from a molecular species in solution, resulting in oxidation of that species (e.g., halides, organometallic complexes, arenes).[8] Because the reduction of $S_2O_8^{2-}$ results in the oxidation of a molecule in solution, we refer to this electrochemical reaction sequence as *reductive oxidation*. In contrast to $S_2O_8^{2-}$, the one-electron oxidation of $C_2O_4^{2-}$ yields the transient $C_2O_4^{\bullet-}$ that rapidly dissociates to CO_2 and the highly reducing carbon dioxide radical anion ($E^{0\prime}$ ($CO_2^{\bullet-}/CO_2$) = –2.1 V vs. Ag/AgCl (3.5 M KCl)).[9, 10] Electrogenerated $CO_2^{\bullet-}$ can undergo a subsequent 1*e* oxidation at the working electrode or can be used to reduce a solution species. Hence, the electrochemical reaction sequence is referred to as *oxidative reduction*.

The short-lived intermediates $S_2O_8^{3\bullet-}$ ($\tau_{1/2}$ ~ 5 ps)[12] and $C_2O_4^{\bullet-}$ ($\tau_{1/2}$ ~ 1 μs)[11] decompose to $SO_4^{\bullet-}$ and $CO_2^{\bullet-}$ respectively, in close vicinity to the electrode surface and can be rapidly reduced to SO_4^{2-} or oxidized to CO_2, respectively. Consequently, direct oxidation of $C_2O_4^{2-}$ or reduction

of $S_2O_8^{2-}$ generates low amounts of $CO_2^{\bullet-}$ and $SO_4^{\bullet-}$ in solution, respectively, that can be used to carry out synthetic transformations (left side of Figure 1B and 1C). To avoid the oxidation of $CO_2^{\bullet-}$ and reduction of $SO_4^{\bullet-}$ at the electrode surface, an outer-sphere redox mediator (i.e., species A in Figure 1B and 1C) is required to reduce $S_2O_8^{2-}$ and oxidize $C_2O_4^{2-}$. In contrast with the direct reactions of these species at the electrode, the use of a mediator yields $SO_4^{\bullet-}$ and $CO_2^{\bullet-}$ several 10s of micrometers from the working electrode,[12] where they can be intercepted by organic compounds for synthetic purposes.

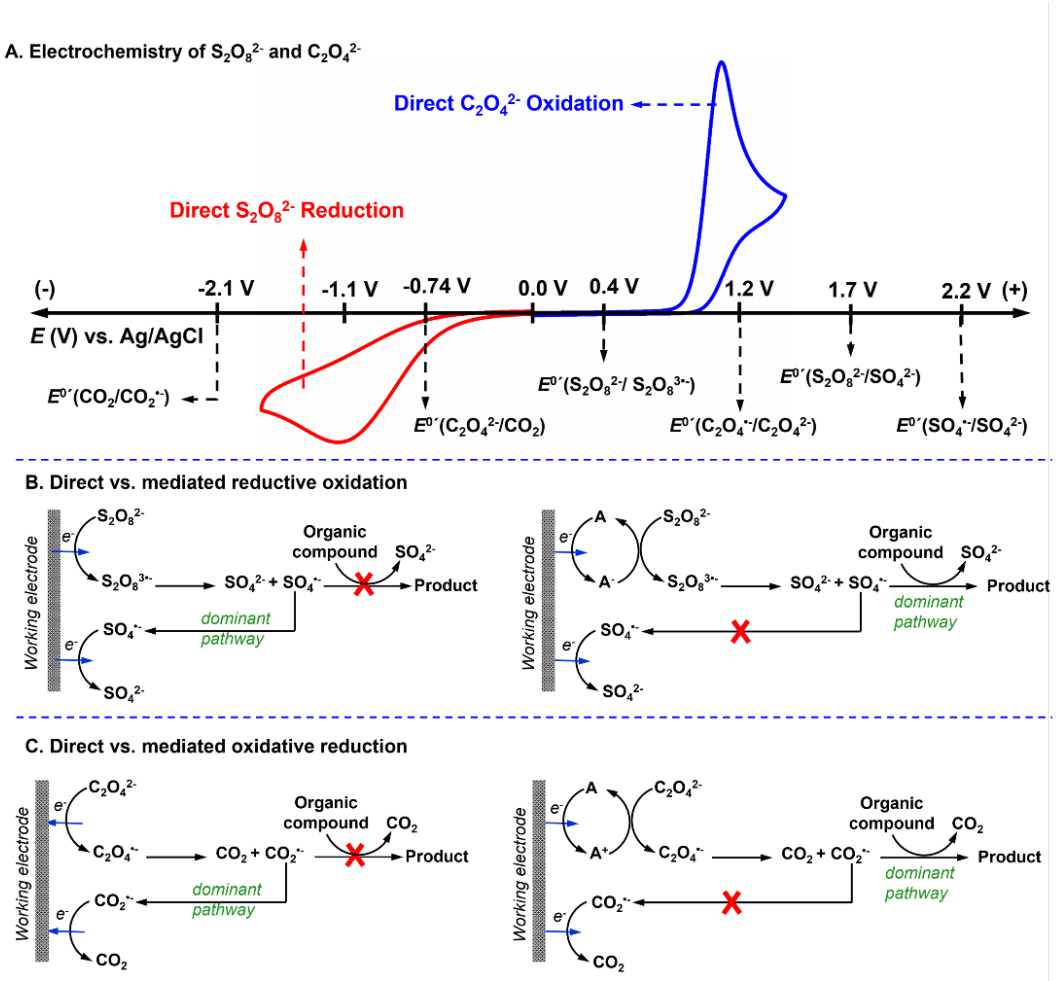

Figure 1. (A) Cyclic voltammetry in an O_2-free aqueous solution containing 5.0 mM $Na_2S_2O_8$ (red trace), 5.0 mM $Na_2C_2O_4$ (blue trace) and 0.1 M Na_2SO_4 (pH = 6.8). Schematic of direct vs. mediated mechanisms for the (B) reductive oxidation and (C) oxidative reduction processes. Voltammograms were recorded at a

scan rate (ν) of 100 mV/s using a 0.07 cm^2 GC working electrode, a Pt mesh auxiliary electrode, and a Ag/AgCl (3.5 M KCl) reference electrode.

$S_2O_8^{2-}$ is widely employed in (non-electrochemical) organic synthesis. $SO_4^{\bullet-}$, generated by heat or light, is an efficient reagent for the hydrogen atom abstraction from organic compounds, and there are several reports where $S_2O_8^{2-}$ is utilized for C–H activation reactions.[13-15] In contrast, to the best of our knowledge, $C_2O_4^{2-}$ has never been utilized for synthetic purposes. Rather, the $CO_2^{\bullet-}$ is typically generated from formate oxidation.[16–18] Recent reports show that photochemically generated $CO_2^{\bullet-}$ can be used to reductively cleave the C–Cl moiety in electron-deficient chloroarenes[16, 17] or in hydrocarboxylation reactions.[18] In both cases, however, an organic solvent was employed to carry out the chemical reaction, and the $SO_4^{\bullet-}$ and $CO_2^{\bullet-}$ were generated using light or heat.

Herein, we describe our recent efforts to apply the mediated electrochemical reduction of $S_2O_8^{2-}$ by electrogenerated hexaammineruthenium(II) ($Ru(NH_3)_6^{2+}$) to carry out C–H activation of benzyl alcohol and toluene in aqueous solution. Additionally, we describe preliminary studies of the mediated electrooxidation of oxalate using tris(bipyridine)ruthenium(III) ($Ru(bpy)_3^{3+}$) to form $CO_2^{\bullet-}$ in an aqueous solution. Electrogenerated $CO_2^{\bullet-}$ is used for the homogeneous reduction of the C–Br moiety in benzyl bromide and for the reduction of Zn^{2+} in an aqueous solution.

Results and Discussion

The direct reduction of $S_2O_8^{2-}$ and rapid dissociation of $S_2O_8^{2-}$ produces $SO_4^{\bullet-}$ within ~10 nm of the GC electrode. Therefore, the direct reduction of the $SO_4^{\bullet-}$ at the GC electrode occurs prior to being intercepted by an organic compound. Several outer-sphere mediators were explored for the homogeneous reduction of $S_2O_8^{2-}$. Figure 3 shows the cyclic voltammetry (CV) of the GC electrode in solutions containing nitrobenzene (NB), hexaammineruthenium(III) chloride

($Ru(NH_3)_6^{3+}$), potassium hexacyanoferrate(III) ($Fe(CN)_6^{3-}$), and potassium hexachloroiridate(III) ($[IrCl_6]^{3-}$) in the presence and absence of $S_2O_8^{2-}$. All four mediators show chemically and thermodynamically reversible 1*e* reduction behavior in the absence of $S_2O_8^{2-}$. Upon addition of $S_2O_8^{2-}$, the voltammetric responses of $[IrCl_6]^{3-}$ and $Fe(CN)_6^{3-}$ remain unchanged. On the other hand, the CVs of $Ru(NH_3)_6^{3+}$ and NB in the presence of $S_2O_8^{2-}$ show an increase in the cathodic peak current, concurrent with the disappearance of the reverse anodic peak. These results indicate that the electrogenerated $Ru(NH_3)_6^{2+}$ and NB radical anion are both capable of reducing $S_2O_8^{2-}$, presumably by a 1*e* transfer. In comparison with nitrobenzene, $Ru(NH_3)_6^{2+}$ reduces $S_2O_8^{2-}$ at a less negative potential and generates a larger electrocatalytic current. Therefore, $Ru(NH_3)_6^{3+}$ was selected as the electrocatalyst to homogenously generate $SO_4^{\bullet-}$ for the subsequent electroorganic reactions. We also note that $Ru(NH_3)_6^{2+}$ reduces $S_2O_8^{2-}$ at potentials approximately 0.5 V more positive than where $S_2O_8^{2-}$ is directly reduced at GC. Thus, $Ru(NH_3)_6^{2+}$ acts as an efficient electrocatalyst for $S_2O_8^{2-}$ reduction, generating $SO_4^{\bullet-}$ in the solution at potentials where $S_2O_8^{2-}$ is not directly reduced at the GC electrode. This combination of properties ensures that $SO_4^{\bullet-}$ is available for synthetic purposes, as shown on the right-side column of Figure 1B.

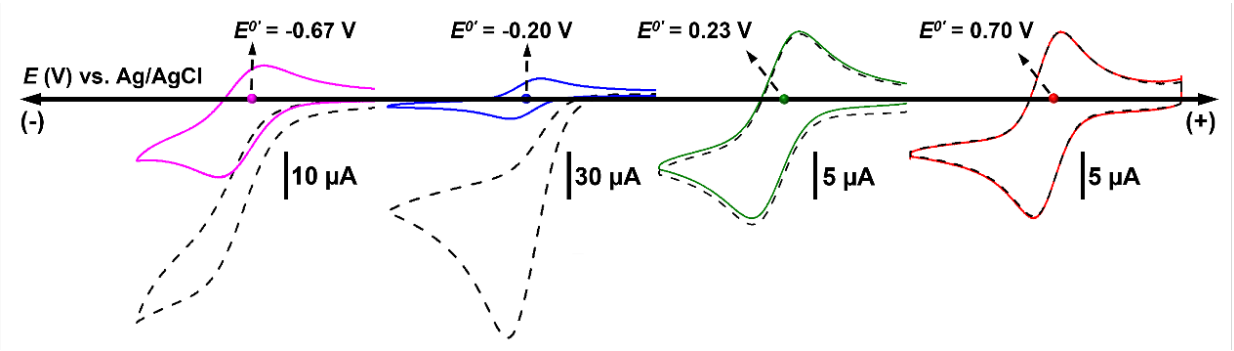

Figure 2. Cyclic voltammetry of 0.5 mM (magenta) NB, (blue) $Ru(NH_3)_6^{3+}$, (green) $Fe(CN)_6^{3-}$, and (red) $[IrCl_6]^{3-}$ in an O_2-free aqueous solution, in the absence and presence of 5 mM $Na_2S_2O_8$ (dashed black trace). Voltammograms were recorded at a scan rate (ν) of 100 mV/s using a 0.07 cm^2 GC working electrode, a Pt

mesh auxiliary electrode, and a Ag/AgCl (3.5 M KCl) reference electrode. The solution contained 0.1 M Na_2SO_4 (pH = 6.8).

Figure 3 shows the variation of the height of the cathodic peak upon addition of 2.0 mM benzyl alcohol (**BA**) to a solution containing 0.5 mM $Ru(NH_3)_6^{3+}$ and 4.5 mM $S_2O_8^{2-}$.[12] The dependence of the cathodic peak current as function of **BA** concentration is shown in Figure 3B. We have previously proposed a five-step mechanism for the electrocatalytic reduction of $S_2O_8^{2-}$ via $Ru(NH_3)_6^{3+}$ (eq. 1–5) based on CV analysis. The 1*e* reduction of $Ru(NH_3)_6^{3+}$ yields $Ru(NH_3)_6^{2+}$ (eq. 1), which homogeneously reduces $S_2O_8^{2-}$ resulting in the regeneration of $Ru(NH_3)_6^{3+}$ and the generation of $S_2O_8^{3\bullet-}$ (eq. 2). Electrogenerated $S_2O_8^{3\bullet-}$ dissociates rapidly (i.e., $\tau_{1/2} < 5$ ps) forming SO_4^{2-} and $SO_4^{\bullet-}$. Finally, $SO_4^{\bullet-}$ reduces by 1*e* either via homogeneous reduction by $Ru(NH_3)_6^{2+}$ (eq. 4) or directly at the working electrode (eq. 5).

$$Ru(NH_3)_6^{3+} + e^- \rightleftharpoons Ru(NH_3)_6^{2+} \quad (1)$$

$$Ru(NH_3)_6^{2+} + S_2O_8^{2-} \rightleftharpoons Ru(NH_3)_6^{3+} + S_2O_8^{3\bullet-} \quad (2)$$

$$S_2O_8^{3\bullet-} \rightleftharpoons SO_4^{2-} + SO_4^{\bullet-} \quad (3)$$

$$Ru(NH_3)_6^{2+} + SO_4^{\bullet-} \rightleftharpoons Ru(NH_3)_6^{3+} + SO_4^{2-} \quad (4)$$

$$SO_4^{\bullet-} + e^- \rightleftharpoons SO_4^{2-} \quad (5)$$

The decrease of the cathodic peak height (i.e., i_{pc}) in the presence of BA is results from $SO_4^{\bullet-}$ abstracting a hydrogen atom from benzyl alcohol to form the corresponding benzyl alcohol radical (**BAR**) (eq. 6). The BAR can then be oxidized to yield benzaldehyde (**BAL**) via reaction with $SO_4^{\bullet-}$ (eq. 7) or $Ru(NH_3)_6^{3+}$ (eq. 8). A direct consequence of eqs. 6 and 7 is the homogenous conversion of $SO_4^{\bullet-}$ to SO_4^{2-} in solution rather than at the electrode. Thus, i_{pc} decreases with increasing concentration of BA, as shown in Figure 3B.

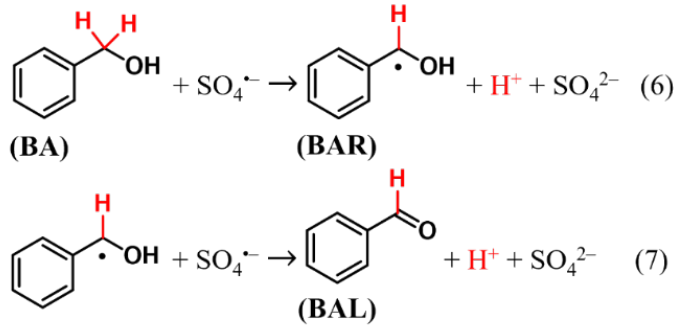

$$+ SO_4^{\bullet-} \rightarrow + H^+ + SO_4^{2-} \quad (6)$$

$$+ SO_4^{\bullet-} \rightarrow + H^+ + SO_4^{2-} \quad (7)$$

$$Ru(NH_3)_6^{3+} + \textbf{BAR} \rightarrow Ru(NH_3)_6^{2+} + H^+ + \textbf{BAL} \quad (8)$$

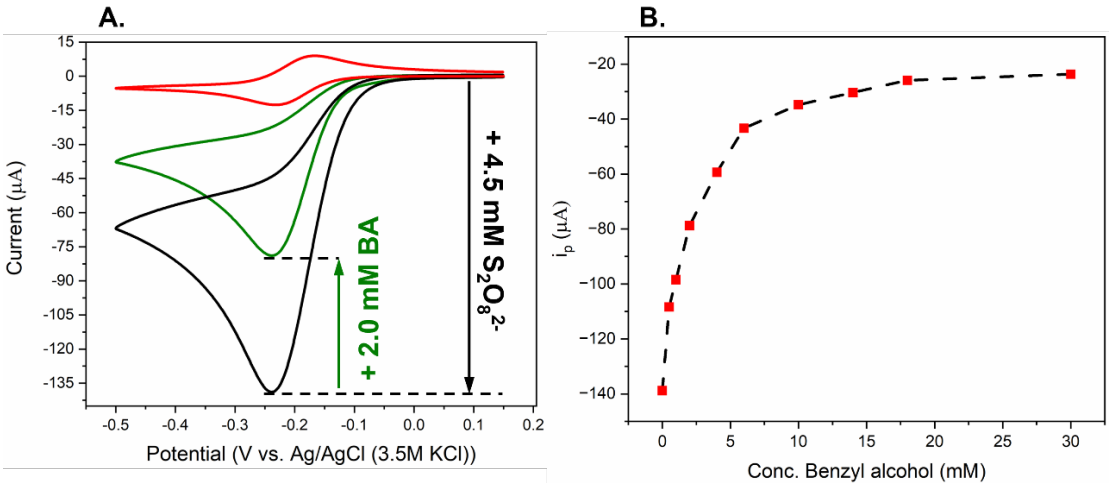

Figure 3. (A) Cyclic voltammetric response in an O_2-free H_2O-MeCN solution (80% H_2O v/v) containing (red) 0.50 mM $Ru(NH_3)_6^{3+}$, (black) 0.50 mM $Ru(NH_3)_6^{3+}$and 4.5 mM $S_2O_8^{2-}$, and (green) 0.50 mM $Ru(NH_3)_6^{3+}$, 4.5 mM $S_2O_8^{2-}$, and 2.0 mM **BA**. (B) Cathodic peak current (i_{pc}) versus the concentration of benzyl alcohol. Voltammograms were recorded at a scan rate (v) of 100 mV/s using a 0.07 cm^2 GC working electrode, a Pt mesh auxiliary electrode, and a Ag/AgCl (3.5 M KCl) reference electrode. The solution contained 0.1 M Na_2SO_4 (pH = 6.8).

The utility of the $Ru(NH_3)_6^{3+}/S_2O_8^{2-}$ system for the electrochemical oxidation of BA was examined via constant potential electrolysis at –0.5 V vs. Ag/AgCl (3.5 M KCl) in a divided cell, using a reticulated vitreous carbon (RVC) disk as the working electrode.[12] The scope of the aliphatic and benzylic alcohol oxidation via mediated reductive oxidation is shown in Figure 4A. Mediated reductive oxidation of various alcohols in neutral pH (i.e., pH = 6.8) yields

aldehydes/ketones whereas electrolysis in basic pH (i.e., pH = 12.5) predominately yields carboxylic acids.

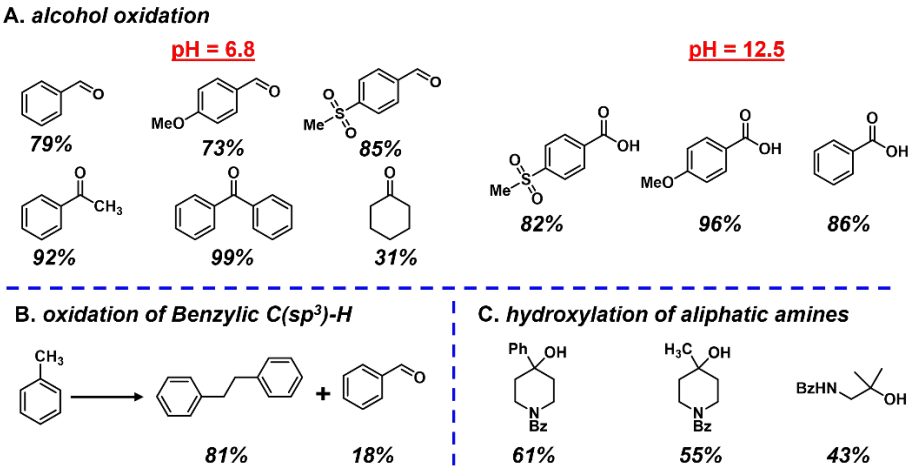

Figure 4. Utility of reductive oxidation for: (A) selective oxidation of aliphatic and benzylic alcohols; (B) oxidation of benzylic C(sp^3)–H; and (C) hydroxylation of aliphatic amines. Constant potential electrolysis was performed at –0.5 V vs. Ag/AgCl (3.5 M KCl) in an O_2-free H_2O-MeCN solution (80% H_2O v/v) containing 0.1 M Na_2SO_4 using a divided cell. In (A) and (C), a RVC disk was employed as the working electrode, whereas in (B) a graphite rod working electrode was used.

Electrochemical reductive oxidation of BA is an example of benzylic C(sp^3)–H activation via electrogenerated $SO_4^{\bullet-}$. In preliminary experiments, we examined the utility of reductive oxidation toward activation of the inert benzylic C(sp^3)–H bond. In this context, toluene was selected as the model compound. The benzylic C–H activation of toluene is typically carried out using photochemical methods.[19,20] As shown in Figure 5A, the peak potential for the direct oxidation of toluene overlaps with the onset of water oxidation. Therefore, any attempt to directly oxidize toluene at E > 1.95 V vs. Ag/AgCl (3.5 M KCl) in an aqueous solution results in water oxidation. However, reductive oxidation via reduction of $S_2O_8^{2-}$ at negative potentials allows for toluene oxidation. Upon addition of 5.0 mM toluene to an aqueous solution containing 0.5 mM $Ru(NH_3)_6^{3+}$ and 3.0 mM $S_2O_8^{2-}$, the height of the cathodic peak decreases (Figure 5B). In the

absence of toluene, electrogenerated $SO_4^{\bullet-}$ is reduced by $Ru(NH_3)_6^{2+}$ (i.e., eq. 4) or directly at the working electrode (i.e., eq. 5). However, electrogenerated $SO_4^{\bullet-}$ homogeneously oxidizes toluene, which manifests itself as a decrease in the cathodic peak current, suggesting that reductive oxidation enables toluene oxidation in aqueous solution. Electrolysis of 5.0 mM toluene was carried out in the presence of 1.0 mM $Ru(NH_3)_6^{3+}$ and 25 mM $S_2O_8^{2-}$ at a constant potential of –0.5 V vs. Ag/AgCl (3.5 M KCl). Electrolysis was performed in a divided cell containing an O_2-free solution of H_2O-MeCN (80% v/v H_2O) using a graphite rod as the working electrode. Analysis of the product distribution revealed that ~ 80% of the toluene was oxidized to bibenzyl, and ~ 17% of the toluene was converted to benzaldehyde as the result of overoxidation via $SO_4^{\bullet-}$ (Figure 4B).

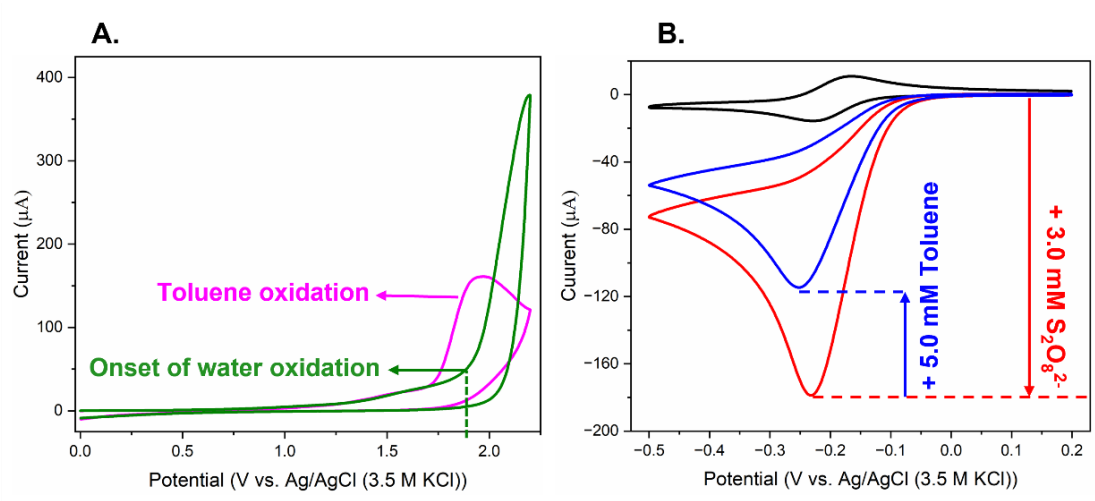

Figure 5. (A) Cyclic voltammetry in the absence (green) and presence of 5.0 mM toluene (magenta). (B) CVs of a solution containing: (black) 0.50 mM $Ru(NH_3)_6^{3+}$; (red) 0.50 mM $Ru(NH_3)_6^{3+}$and 4.5 mM $S_2O_8^{2-}$; and (blue) 0.50 mM $Ru(NH_3)_6^{3+}$, 4.5 mM $S_2O_8^{2-}$, and 2.0 mM BA. All CVs were recorded using a 0.07 cm^2 GC working electrode, a Pt mesh auxiliary electrode, and a Ag/AgCl (3.5 M KCl) reference electrode. The measurements were made at ν = 100 mV/s in an O_2-free H_2O/MeCN solution (80% H_2O v/v) containing 0.1 M Na_2SO_4 (pH = 6.5).

We also have examined the oxidation of the remote C–H bond in aliphatic amines to better understand the utility of mediated reductive oxidation for activation of a remote C(sp^3)–H bond. The oxygenation of aliphatic amines was carried out previously by Sanford and coworkers via

thermal activation of $S_2O_8^{2-}$ to functionalize remote C(sp^3)–H in a dilute H_2SO_4 solution.[21] This homogenous chemical process was shown to have a high yield and to be applicable to a large scope of substrates.

Electrochemical hydroxylation was carried out at constant potential of –0.5 V vs. Ag/AgCl in a phosphate buffer solution (pH = 3.1) containing 1.0 mM $Ru(NH_3)_6^{3+}$, 30 mM $S_2O_8^{2-}$, and 5.0 mM of an aliphatic amine. As shown in Figure 4C, three aliphatic amines were hydroxylated at the para position, suggesting the utility of mediated reductive oxidation for remote activation of the C–H moiety and the subsequent hydroxylation reaction.

Analogous to the use of $S_2O_8^{2-}$ reduction for carrying out oxidations, $C_2O_4^{2-}$ oxidation can be used for performing reduction of organic species. The direct oxidation of $C_2O_4^{2-}$ ($E^{0'}$ ($C_2O_4^{\bullet-}$ $C_2O_4^{2-}$) = 1.2 vs Ag/AgCl (3.5 M KCl)) results in the formation of the $CO_2^{\bullet-}$ very close to the electrode surface (< 1 μm), which results in the preferential oxidation of the $CO_2^{\bullet-}$ at the electrode rather than in solution with a reaction partner.[11] To circumvent this problem, a redox mediator can be used to generate $CO_2^{\bullet-}$ further away from the electrode surface. Potassium hexachloroiridate(II) ($[IrCl_6]^{4-}$), tris(2,2'-bipyridine)iron(II) tetrafluoroborate ($Fe(bpy)_3^{2+}$), and tris(2,2'-bipyridine)ruthenium(II) chloride ($Ru(bpy)_3^{2+}$) were screened for the ability of their oxidized forms to oxidize $C_2O_4^{2-}$ (Figure 6). In general, as $E^{0'}$ of the metal-based mediator becomes more positive, the rate of mediation increases, in agreement with prior results reported by Bard and co-workers.[22] As shown in Figure 6A, a minimal increase in the anodic peak current for $[IrCl_6]^{4-}$ oxidation occurs upon addition of $C_2O_4^{2-}$, indicating that transfer of an electron from $C_2O_4^{2-}$ to $[IrCl_6]^{3-}$ is negligible. Upon addition of $C_2O_4^{2-}$ to a solution containing $Fe(bpy)_3^{2+}$, a sigmoidal CV shape representative of sluggish homogeneous electron transfer is observed, as previously

reported.[22] However, the CV of $Ru(bpy)_3^{2+}$ in the presence of $C_2O_4^{2-}$ shows that electrogenerated $Ru(bpy)_3^{3+}$ can rapidly accept an electron from $C_2O_4^{2-}$, in agreement with previous reports.[22]

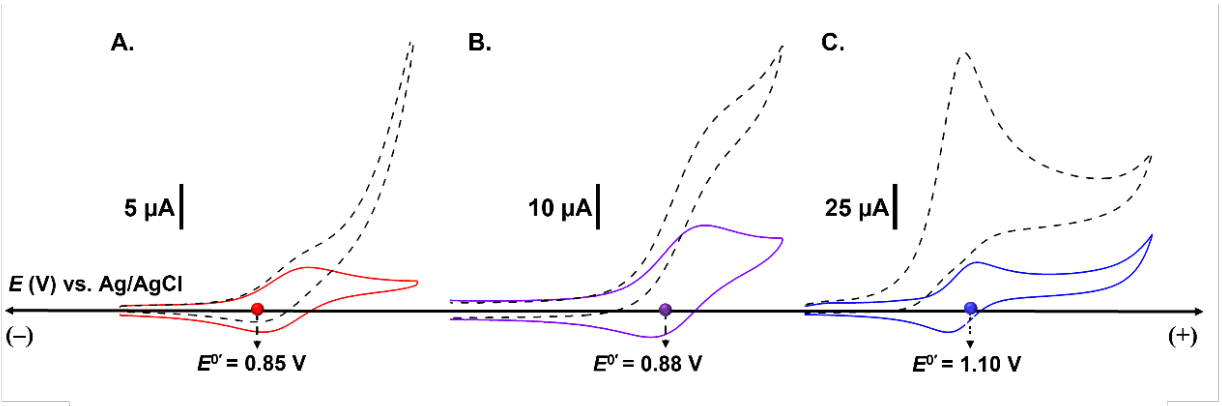

Figure 6. Cyclic voltammetry of in an O_2-free H_2O/MeCN solution (90% H_2O v/v) containing 0.1 M PBS (pH = 7.3) with (red) 1.0 mM $IrCl_6^{4-}$; (violet) $Fe(bpy)_3^{2+}$; and (blue) $Ru(bpy)_3^{2+}$, in the absence and presence of 2.0 mM $C_2O_4^{2-}$ (dashed black traces). All CVs were recorded using a 0.07 cm^2 GC working electrode, a Pt mesh auxiliary electrode, and a Ag/AgCl (3.5 M KCl) reference electrode. The measurements were made at ν = 10 mV/s.

The $Ru(bpy)_3^{2+}/C_2O_4^{2-}$ system was used to generate the $CO_2^{\bullet-}$ for the reduction of benzyl bromide and Zn^{2+} ions. Figure 7A shows a decrease in the anodic peak current for $Ru(bpy)_3^{2+}$ oxidation upon addition of 3.0 mM benzyl bromide to a solution of 1.0 mM $Ru(bpy)_3^{2+}$ and 2.0 mM $C_2O_4^{2-}$. Based on the reported ECL mechanism for the $Ru(bpy)_3^{2+}/C_2O_4^{2-}$ system along with analysis of the CV of $Ru(bpy)_3^{2+}$ in the presence of $C_2O_4^{2-}$, a 7-step mechanism for the oxidation of $C_2O_4^{2-}$ by electrogenerated $Ru(bpy)_3^{3+}$ (eq. 9–15) is proposed to occur.[22, 23] Briefly, $Ru(bpy)_3^{3+}$ is produced from the 1*e* oxidation of $Ru(bpy)_3^{2+}$ (eq. 9). Then, $Ru(bpy)_3^{3+}$ homogeneously oxidizes $C_2O_4^{2-}$ to yield $C_2O_4^{\bullet-}$ (eq. 10), which rapidly decomposes (i.e., $\tau_{1/2} \approx 1$ μs) into CO_2 and $CO_2^{\bullet-}$ (eq. 11). The $CO_2^{\bullet-}$ in solution can reduce $Ru(bpy)_3^{3+}$ to $Ru(bpy)_3^{2+}$ (eq. 12), reduce $Ru(bpy)_3^{2+}$ to $Ru(bpy)_3^{+}$ (eq. 13), or be oxidized to CO_2 at the electrode (eq. 14). Any $Ru(bpy)_3^{+}$ that is formed will react with $Ru(bpy)_3^{3+}$ to generate two equivalents of $Ru(bpy)_3^{2+}$ (eq. 15).[23]

$Ru(bpy)_3^{2+} \rightleftharpoons Ru(bpy)_3^{3+} + e^-$ (9)

$Ru(bpy)_3^{3+} + C_2O_4^{2-} \rightleftharpoons Ru(bpy)_3^{2+} + C_2O_4^{\bullet-}$ (10)

$C_2O_4^{\bullet-} \rightleftharpoons CO_2 + CO_2^{\bullet-}$ (11)

$Ru(bpy)_3^{3+} + CO_2^{\bullet-} \rightleftharpoons Ru(bpy)_3^{2+} + CO_2$ (12)

$Ru(bpy)_3^{2+} + CO_2^{\bullet-} \rightleftharpoons Ru(bpy)_3^{+} + CO_2$ (13)

$CO_2^{\bullet-} \rightleftharpoons CO_2 + e^-$ (14)

$Ru(bpy)_3^{3+} + Ru(bpy)_3^{+} \rightleftharpoons 2Ru(bpy)_3^{2+}$ (15)

An alternative reaction pathway for the $CO_2^{\bullet-}$ becomes available upon the addition of benzyl bromide to the $Ru(bpy)_3^{2+}/C_2O_4^{2-}$ system (eq. 16) wherein the C–Br bond contained in benzyl bromide is reductively cleaved via a homogeneous one-electron transfer from $CO_2^{\bullet-}$. In the absence of benzyl bromide, the $CO_2^{\bullet-}$ acts to regenerate the primary current-contributing species, $Ru(bpy)_3^{2+}$ (eq. 12–14). In the presence of benzyl bromide, however, the $CO_2^{\bullet-}$ is intercepted (i.e., eq. 16), thereby avoiding the occurrence of eqs. 12–15, which leads to the decrease in anodic peak current (i_{pa}) observed in Figure 7A. In very preliminary studies, the electrolysis of the $Ru(bpy)_3^{2+}/C_2O_4^{2-}$ system in the presence of benzyl bromide predominately gives benzaldehyde as the major product. Although this result demonstrates the capability of $CO_2^{\bullet-}$ to reductively cleave the benzylic C–Br moiety, a net oxidation occurs. At the potential required to generate $CO_2^{\bullet-}$, the benzylic radical shown in eq. 16 and Br^- can both undergo heterogeneous oxidation to generate a benzylic cation and Br_2.[24] The oxygen contained in the product likely originates from water, which can act as a nucleophile to add to the electrophilic benzylic cation. This yields benzyl alcohol that is either oxidized at the electrode (or by Br_2) to give the product, benzaldehyde. Oxidative reduction reactivity can also be applied to the reduction of zinc ions (eq. 17) ($E^{0'}$

(Zn^{2+}/Zn) = –0.95 V vs. Ag/AgCl (3.5 M KCl)), where two equivalents of electrogenerated $CO_2^{\bullet-}$ reduce Zn^{2+} to neutral zinc metal (Figure 7B). Although it is hypothesized that Zn^0 is formed in this reaction, isolation and analysis of product following bulk electrolysis is still required.

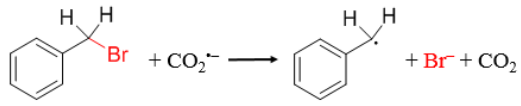

(16)

$$Zn^{2+} + 2CO_2^{\bullet-} \rightarrow Zn^0 + 2CO_2 \qquad (17)$$

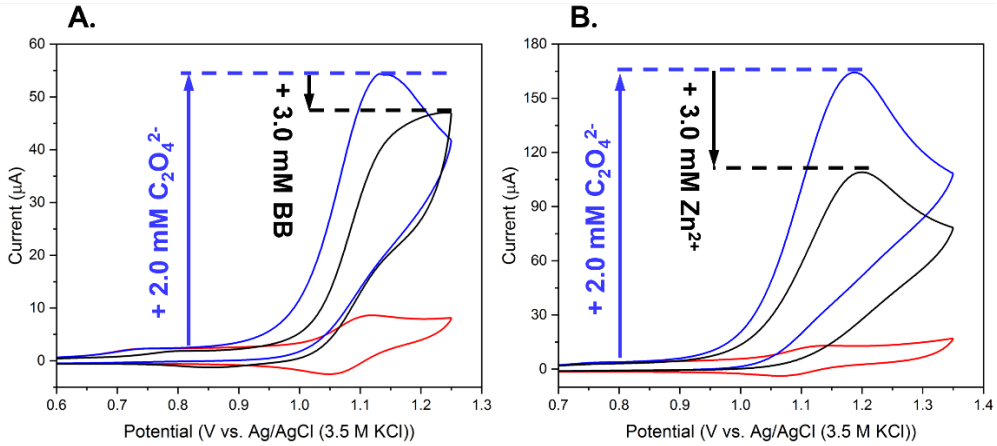

Figure 7. (A) Cyclic voltammetry in solutions containing: (red) 0.50 mM $Ru(bpy)_3^{2+}$; (blue) 0.50 mM $Ru(bpy)_3^{2+}$ and 2.0 mM $C_2O_4^{2-}$; and (black) 0.50 mM $Ru(bpy)_3^{2+}$, 2.0 mM $C_2O_4^{2-}$, and 3.0 mM benzyl bromide. (B) Cyclic voltammetry in solutions containing: (red) 0.50 mM $Ru(bpy)_3^{2+}$; (blue) 0.50 mM $Ru(bpy)_3^{2+}$, and 5.0 mM $C_2O_4^{2-}$; and (black) 0.50 mM $Ru(bpy)_3^{2+}$, 5.0 mM $C_2O_4^{2-}$, and 3.0 mM $ZnCl_2$. Voltammogram A was recorded in a H_2O/MeCN solution (90% H_2O v/v) containing 0.1 M PBS (pH = 7.3), and B was recorded in an aqueous solution containing 0.1 M PBS (pH = 7.3). All CVs were carried out with a 0.07 cm^2 GC working electrode, a Pt mesh auxiliary electrode, and a Ag/AgCl (3.5 M KCl) reference electrode at ν = 100 mV/s in O_2-free solutions.

Tri-*n*-propylamine (TPA) also presents an opportunity to conduct oxidative reduction as its oxidation gives rise to a strong reducing agent. The electrochemical behavior of TPA has been studied previously.[25] When TPA is oxidized, the $TPA^{\bullet+}$ ($\tau_{1/2} \approx 1$ ms) is rapidly deprotonated to yield $TPA^{\bullet}$ ($E^{0'}$ ($TPA^{\bullet}/TPA^{-}$) = –1.7 V vs. Ag/AgCl (3.5 M KCl)), which is then capable of

homogeneously reducing organic compounds. Based on the half-life for the $TPA^{\bullet+}$, the $TPA^{\bullet}$ is predicted to be generated approximately 1 μm from the electrode surface where it is susceptible to oxidation. Voltammetric analysis of TPA in the presence of 2,2,6,6-tetramethyl-1-piperidinyloxy (TEMPO) demonstrates that the oxidized form of TEMPO acts as an electrocatalyst for TPA oxidation (Figure 8A). Thus, TEMPO was used to mediate TPA oxidation to form $TPA^{\bullet}$ further from the electrode. Then, upon introduction of benzyl bromide to the TEMPO/TPA system, a decrease in peak current was observed, characteristic of oxidative reduction chemistry (Figure 8 B).

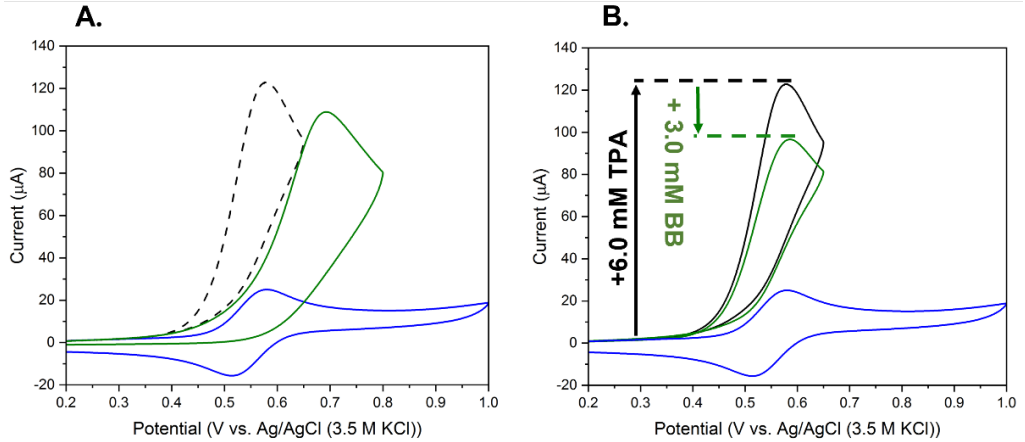

Figure 8. (A) Cyclic voltammetry in O_2-free H_2O/MeCN (90% H_2O v/v) solutions containing: (blue) 1.0 mM TEMPO; (green) 6.0 mM TPA; and (black dashed line) 1.0 mM TEMPO and 6.0 mM TPA. (B) Cyclic voltammetry in O_2-free H_2O/MeCN (90% H_2O v/v) solutions containing: (blue) 1.0 mM TEMPO; (black) 1.0 mM TEMPO and 6.0 mM TPA; and (green) 1.0 mM TEMPO, 6.0 mM TPA, and 3.0 mM benzyl bromide. All voltammograms were recorded at ν = 100 mV/s using a 0.07 cm^2 GC working electrode, a Pt mesh auxiliary electrode, and a Ag/AgCl (3.5 M KCl) reference electrode. All solutions contained 0.1 M PBS (pH = 10.5).

Conclusion

In this work, we showcased the utility of the electrochemically generated intermediates $SO_4^{\bullet-}$ and $CO_2^{\bullet-}$ to carry out electroorganic reactions close to the water potential window. In both reductive oxidation and oxidative reduction, a mediator was required to produce $CO_2^{\bullet-}$ and $SO_4^{\bullet-}$

away from the working electrode to allow these radical ions to react with the organic substrate. Our analysis shows that $Ru(NH_3)_6^{3+}$ is the optimal electrocatalyst for the homogeneous reduction of $S_2O_8^{2-}$. The mediated reductive oxidation using $Ru(NH_3)_6^{3+}$ and $S_2O_8^{2-}$ was employed to oxidize various benzylic and aliphatic alcohols, toluene, and aliphatic amines at –0.5 V vs. Ag/AgCl in H_2O/MeCN solutions with high yield. Analogous to previous findings, oxalate oxidation can be mediated by $Ru(bpy)_3^{3+}$ to generate $CO_2^{\bullet-}$ in water. The utility of the $CO_2^{\bullet-}$ for electrosynthesis was examined by reductive cleavage of the C–Br moiety in benzyl bromide as well as in the reduction of Zn ions.

Experimental

Cyclic Voltammetry Studies

Cyclic voltammetry studies were carried out using a Biologic Dual Channel SP300 Potentiostat and a three-electrode configuration including a 0.07 cm^2 glassy carbon (GC) working electrode, a Pt mesh auxiliary electrode, and a Ag/AgCl (3.5 M KCl) reference electrode in an undivided cell. The GC electrode was polished with a slurry of 1-μm alumina in H_2O and then dried with stream of N_2.

Controlled-Potential Electrolysis

Controlled-potential electrolysis was performed at room temperature using a Biologic Dual Channel SP300 Potentiostat. A detailed description for the preparation of the electrolysis cell and the electrolysis procedure is outlined elsewhere.[26] An example *i*-t trace for the mediated electrolysis of benzyl alcohol and the sequence of addition of reagents during electrolysis is shown in Figure 9. First, 20 mL of a deoxygenated H_2O-MeCN (80% H_2O v/v) was placed in the cathode compartment of the electrolysis cell. The cathode compartment was maintained under Ar for the duration of the electrolysis. Next, a constant potential of –0.5 V vs Ag/AgCl (3.5 M KCl) was

applied to the cell which is marked by a current spike (**1,** Figure 9). Once the charging current reached a steady baseline, benzyl alcohol was dissolved in 2 mL of MeCN and injected into the cathode compartment (**2**, Figure 9). Next, 1 mL of the deoxygenated catholyte was removed from the electrolysis cell and was used to dissolve $Na_2S_2O_8$. The solution of $Na_2S_2O_8$ was then injected into the cathode compartment (**3**, Figure 9). The same procedure was carried out to introduce $Ru(NH_3)_6^{3+}$ into the electrolysis cell. A current spike was observed upon injection of $Ru(NH_3)_6^{3+}$ to the cathode compartment of the electrolysis cell (**4**, Figure 9). The electrolysis was concluded once the current returned to the baseline level and remained steady for ~15 min (**5**, Figure 9).

A similar procedure was carried out for mediated reductive oxidation of benzylic and aliphatic alcohols, toluene, aliphatic amines, and benzyl bromide. Electrolyses of aliphatic amines were carried out in an aqueous phosphate buffer (pH = 3.10). Electrolysis of benzyl bromide was carried out at E_{app} = 1.2 V vs. Ag/AgCl (3.5 M KCl) using $Ru(bpy)_3^{3+}$ as the mediator for oxalate oxidation.

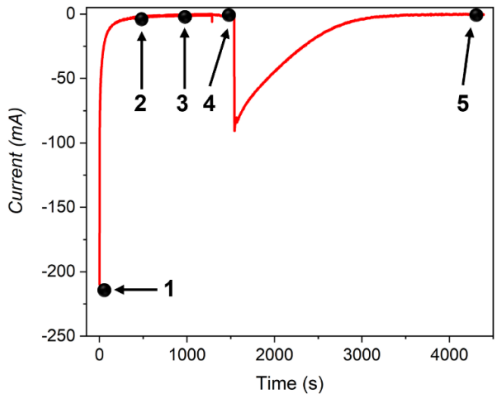

Figure 9. The sequence of events of in mediated electrolysis including: (1) applying –0.5 V vs. Ag/AgCl, (2) injecting benzyl alcohol, (3) introduction of $S_2O_8^{2-}$, (4) injection of $Ru(NH_3)_6^{3+}$, and (5) end of the electrolysis.

Product Isolation

A similar procedure was carried out for the product purification and yield determination upon reductive oxidation of benzylic and aliphatic alcohols, toluene, and benzyl bromide.[12] In

summary, the catholyte was mixed with 20 mL of brine solution and 30 mL of ethyl acetate in a separatory funnel, and the mixture was shaken vigorously. The mixture in the separatory funnel was left to separate into immiscible organic and aqueous layers. Next, the organic phase was removed from the separatory funnel, and the aqueous phase was extracted with ethyl acetate two more times. The three ethyl acetate portions were mixed and dried over anhydrous Na_2SO_4. After one-hour, the dried organic phase was separated from Na_2SO_4 and was condensed under reduced pressure to give a 1-mL organic solution. Next, the components of the organic solution were separated via normal phase chromatography.

Post-electrolysis workup and separation of hydroxylated aliphatic amines followed the procedure reported by Sanford and coworkers.[21] In summary, once electrolysis was complete, the pH of the catholyte was lowered to 1.98 using dropwise additions of dilute H_3PO_4. Next, the catholyte solution was mixed with 20 mL toluene, and the mixture was completely evaporated at 60° C under reduced pressure. The remaining solid in the round bottom flask was mixed with 50 mL MeCN, 12 mL of tri-*n*-ethylamine, and 30 μL of benzoyl chloride. The mixture was stirred at room temperature overnight. Next, MeCN was evaporated under reduced pressure and the solid materials were extracted with 20 mL CH_2Cl_2. Finally, the organic phase was concentrated under reduced pressure to 1-mL, and components of the organic phase were separated using normal phase chromatography.

Acknowledgment

This work was supported by National Science Foundation Center for Synthetic Organic Electrochemistry (CHE-2002158).

References

1 A. J. Bard, R. Parsons and J. Jordan, *Standard Potentials in Aqueous Solution*, Marcel Dekker, New York, 1985.

2 A. J. Bard, L. R. Faulkner and H. S. White, *Electrochemical Methods: Fundamentals and Applications*. John Wiley & Sons, New York, 2022.

3 O. Hammerich and B. Speiser, *Organic electrochemistry*, CRC press, Boca Raton, 2016.

4 A. J. Bard, *Electrogenerated chemiluminescence*. CRC Press, Boca Raton, 2004.

5 A. D. Armstrong, R. E. Huie, W. H. Koppenol, S. V. Lymar, G. Merényi, P. Neta, B. Ruscic, B. D. M. Stanbury, S. Steenken and P. Wardman, *Pure Appl. Chem*., 2015, **87**, 1139.

6 K.C.F. Araújo, E. V. dos Santos, P. V. Nidheesh and C. A. Martínez-Huitle, *Curr. Opin. Chem. Eng.,* 2022, **38**, 100870.

7 R. Memming, *J. Electrochem. Soc.* 1969, **116**, 785.

8 W. -D. Oh, Z. Dong and T. -T. Lim, *Appl. Catal.B,* 2016, **194**, 169.

9 M. -M., Chang, T. Saji and A. J. Bard, *J. Am. Chem. Soc.*, 1977, **99**, 5399.

10 F. Kanoufi, C. Cannes, Y. Zu and A. J. Bard, *J. Phys. Chem. B*, 2001, **105**, 8951.

11 T. Kai, M. Zhou, S. Johnson, S. H. Ahn and A. J. Bard, *J. Am. Chem. Soc*., 2018, **140**, 16178.

12 S. Hosseini, J. N. Janusz, M. Tanwar, A. D. Pendergast, M. Neurock and H. S. White, *J. Am. Chem. Soc.,* 2022, **144**, 21103.

13 H. -Y. Thu, W. -Y. Yu and C. -M. Che, *J. Am. Chem. Soc.,* 2006, **128**, 9048.

14 C. Huang, J. -H. Wang, J. Qiao, X. -W. Fan, B. Chen, C. -H. Tung and L. -Z. Wu, *J. Org. Chem.,* 2019, **84**, 12904.

15 J. Jin and D. W. MacMillan, *Angew. Chem. Int. Ed.,* 2015, **54**, 1565.

16 A. F. Chmiel, O. P. Williams, C. P. Chernowsky, C. P., C. S. Yeung and Z. K. Wickens, *J. Am. Chem. Soc*., 2021, **143**, 10882.

17 C. M. Hendy, G. C. Smith, Z. Xu, T. Zian and N. T. Jui, *J. Am. Chem. Soc.,* 2021, **143**, 8987.

18 S. N. Alektiar and Z. K. Wickens, *J. Am. Chem. Soc.,* 2021, **143**, 13022.

19 D. Mazzarella, G. E. Crisenza and P. Melchiorre, *J. Am. Chem. Soc.*, 2018, **140**, 8439.

20 F. Li, D. Tian, Y. Fan, R. Lee, G. Lu, Y. Yin, B. Qiao, X. Zhao, Z. Xiao and Z. Jiang, *Nat. Commun.*, 2019, **10**, 1774.

21 M. Lee and M. S. Sanford, *Org. Lett.,* 2017, **19**, 572.

22 F. Kanoufi and A. J. Bard, *J. Phys. Chem. B,* 1999, **103**, 10469.

23 I. Rubinstein and A. J. Bard, *J. Am. Chem. Soc*., 1981, **103**, 512.

24 D. D. Wayner, D. McPhee and D. Griller, *J. Am. Chem. Soc.,* 1988, **110**, 132.

25 W. Miao, J. -P. Choi and A. J. Bard*, J. Am. Chem. Soc.*, 2002, **124**, 14478.

26 E. C. R. McKenzie, S. Hosseini, A. G. C. Petro, K. K. Rudman, B. H. R. Gerroll, M. S. Mubarak, A. L. Baker and R. D. Little, *Chem. Rev*., 2022, **122**, 3292.